APPLIED SPECTROSCOPY REVIEWS, 35(4), 255–276 (2000)

Time-Resolved Fluorescence Techniques Applied to Biological Interfaces

A. van Hoek and A. J. W. G. Visser
Wageningen University and Research Centre, Wageningen, The Netherlands

I. INTRODUCTION

All interaction and assembly mechanisms in living matter start at a molecular scale. This fact makes it quite relevant to study and understand the underlying principles of molecular properties. Because of the small (nanometer) scale, the direct observation of molecular mechanisms is never a straightforward matter. Rather complex setups are required in these studies, in which spectroscopy is used as an analytical tool. The molecules under study are subjected to continuous and/or alternating magnetic fields and/or light. The response of the molecular system to that excitation is then detected and analyzed. From the results a molecular model is proposed that is in agreement with the spectroscopic observations. Complementary conclusions can be drawn and the model can be refined by variation of external parameters such as temperature, pressure, molecular concentration, and type of environment or solvent. Depending on the applied stimuli (magnetic fields, photons, etc.), spectroscopic techniques can be divided into magnetic resonance techniques (1) and optical spectroscopy (2).

The spectroscopic techniques discussed in this chapter make use of the absorption of light by molecules. Light absorption brings the molecules instantaneously into an excited state, which is followed by the emission of fluorescence photons in arbitrary directions. Molecular interactions, (radiationless) energy transfer, environment (solvent) dynamics, and structural fluctuations have a direct influence on the fluorescence properties of molecules. These processes can then be described by careful observation and analysis of the fluorescence emission. The study of fluorescence dynamics, in

Reprinted from *Physical Chemistry of Biological Interfaces*, A. Baszkin and W. Norde, ed., Marcel Dekker, Inc., New York, 2000, 651–672.

particular, will provide an extra tool and dimension for the interpretation of fluorescence data. Examples of different excited-state processes that influence the fluorescence dynamics have been schematized in Fig. 1. In Refs. 3 and 4 an extensive overview of fluorescence techniques and a wide range of applications are presented. Numerous other books on fluorescence applications have appeared but are not listed here.

An advantage of the application of fluorescence spectroscopy for studies on biological interfaces is the high sensitivity in combination with the very specific information content. Even the tiniest amount of fluorescence light, the single photon, can be detected. The fluorescence photon carries information on (a) the photon energy, (b) the polarization direction, (c) the timing moment, which can be used to elucidate details of molecular interactions. In some advanced optical spectroscopic techniques, such as coherent anti-Stokes Raman scattering, even the direction of propagation of the emitted photon contains information. In addition to this information content, a large variety of natural and artificial fluorescence probes is available that can be used to investigate a broad range of molecular phenomena (5). These specific fluorescent probes can be incorporated into self-aggregating molecular systems such as mono-, bi-, and multilayers, artificial interfaces, or micelles. The whole system can then be effectively studied using time-resolved fluorescence spectroscopy.

Another important reason to use fluorescence techniques is that molecular processes take place on the same time scale as the fluorescence phenomenon itself. This aspect can be illustrated using the Einstein relation:

$$\langle \Delta x^2 \rangle = 2Dt \tag{1}$$

stating that the mean square root molecular displacement Δx is related to the translational diffusion coefficient D and the traveling time t. If we substitute a time of 150 ns (order of magnitude of the time constant of the fluorescence decay of pyrene) and a diffusion constant $D = 3 \times 10^{-12}\,\mathrm{m^2/s}$ (lateral diffusion over a bilayer membrane), the displacement ($\langle \Delta x^2 \rangle^{1/2}$) is about 1 nm, which is a significant microscopic distance over the surface of such a membrane. This relatively simple example is taken to illustrate that fluorescence spectroscopy is a sensitive method for registering dynamic events in biological systems.

The information retrieved from molecules can be even more specific when the influence of their environment can be modulated, minimized, or well described. Alternatively, the heterogeneity of the spectroscopic data (and thus the complexity) can be reduced by minimizing the number of molecules under study. Examples are (a) the loading of single molecules in a host matrix with silent spectroscopic properties; (b) using an ultrasmall experimental volume by applying evanescent-field, near-field, or multiphoton excitation; or (c) decreasing the concentration of molecules in solution or other matrices. The application of site-selective excitation and the freezing of thermal movements are other methods. One should keep in mind, however, that it is not always realistic to cool biological samples down to cryogenic temperatures, because their properties might be drastically altered.

Fluorescence investigations of interfaces and microemulsions require extra attention to the experimental conditions. In a fluorescence experiment with molecules in transparent and clear solution in a standard cuvette, the position of the effective measurement volume is chosen such that it is well separated from the cuvette walls.

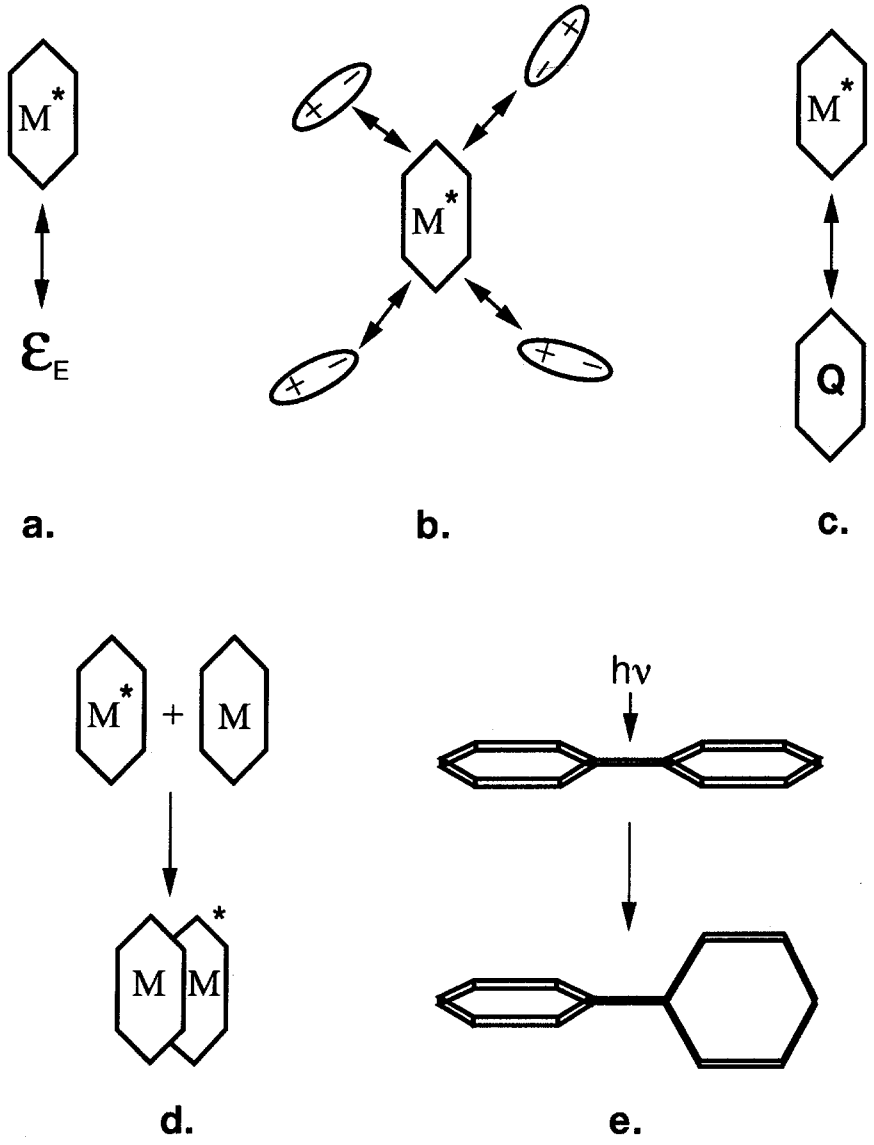

Fig. 1 The decay time of fluorescence of a chromophore can be influenced by different factors, for instance, the dielectric properties ε_E of the environment of the chromophore (a), polarity interactions of the excited molecule with the environment (b), interaction of the chromophore with a quencher molecule (c), excimer formation (d), or conformational changes of the excited molecule upon excitation (e), and that again may influence the fluorescence dynamics. All these different molecular effects can be studied by careful registration and analysis of fluorescence dynamics.

The reason is that one should avoid detection of fluorescence of probe molecules that may interact with the cuvette walls or fluorescence components from other objects or scatter. Therefore the experimental conditions must be adapted when fluorescence measurements are carried out at interfaces or in emulsions. In the case of emulsions, front surface excitation and detection should be applied to avoid artifacts from scattered light in both excitation and detection pathways. Scattering has a direct influence on the polarization properties of that light. In the case of interface studies, not only should the interaction of the fluorescent molecules with the interface be investigated and included in the applied physical model but also the surfaces should be scrupulously cleaned to avoid impurity fluorescence.

II. TIME-RESOLVED SPECTROSCOPIC TECHNIQUES

In this section the time-resolved fluorescence techniques for the study of biological interfaces are briefly explained. The design of different fluorescence probes is very important in the application of fluorescence spectroscopy. In principle, the design should be such that the system under investigation is minimally perturbed after introduction of the fluorescent marker. The spectroscopic methods discussed here are time-resolved fluorescence quenching, time-resolved fluorescence anisotropy, fluorescence decay measurements, fluorescence resonance energy transfer, multiphoton excitation, and single-molecule fluorescence spectroscopy. A review of these techniques as applied to self-aggregating molecular systems can be found in Ref. 6. In this chapter some recent applications are subsequently discussed. The experimental systems range from adsorbed molecular layers on artificial interfaces; micelles from anionic, cationic or nonionic surfactants; bilayer membranes; lipid monolayers; and reversed micelles to single molecules adsorbed on solid-air interfaces. A summary of time-resolved fluorescence techniques applied to these biological interfaces is provided. Some of our own results will be used as illustrations in this survey.

A. Time-Resolved Fluorescence Quenching

The method of time-resolved fluorescence quenching (TRFQ) is a rapid and popular method for obtaining the size of an aggregate, and it can be considered a classical method. The principle is as follows. Fluorophores and quencher molecules are found to be distributed in the micellar compartments in a Poissonian way. In most applications with aqueous micellar solutions, pyrene has been selected as fluorescent probe because of its long fluorescence lifetime, and alkylpyridinium cations frequently serve as a quencher. In reverse micelles a ruthenium-bipyridyl quencher pair, solubilized in the aqueous core, is often chosen. Methylviologen and potassium hexacyanoferrate(III) can act as quenchers. The quenching occurs only in an intramicellar reaction, because when fluorophore and quencher are in separate micelles, the distance for effective fluorescence quenching is too large. Therefore, by choosing sufficiently low concentrations, both fluorophores and quenchers are supplied from different micelles and collide with each other via intermicellar exchange (see Fig. 2). Depending on the concentration ratios of fluorescent probe and quenching molecules, there is a certain distribution of quenched (short time part of the fluorescence decay) and unquenched fluorophores (long time part of that decay). The flu-

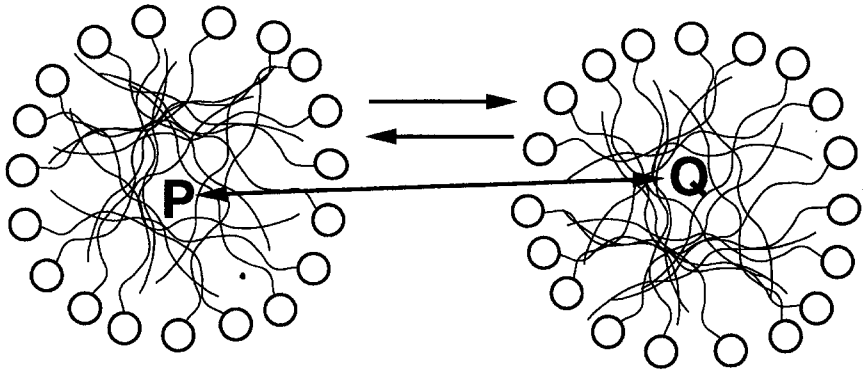

Fig. 2 When chromophores as well as quencher molecules are added to a micellar solution, where both chromophore and quencher prefer the inner environment of the micelle, the probability for quenching is, among other parameters, dependent on the concentration of both components. By using a concentration series and comparing the contributions of the fast part (quenching) and the slow part (no quenching) of the fluorescence decay, the size of the aggregates can be determined (see text for details).

orescence decay $F(t)$ can be modelled by the Infelta-Tachiya equation (7,8):

$$F(t) = A_1 \exp\{-A_2 t + A_3[\exp(-A_4 t) - 1]\} \tag{2}$$

where

$$A_1 = F(0), \text{ the fluorescence intensity at } t = 0$$
$$A_2 = 1/\tau_0 + k_q k_- \langle n \rangle / A_4$$
$$A_3 = k_q^2 \langle n \rangle / A_4^2$$
$$A_4 = k_q + k_-$$

k_q and k_- are the pseudo-first-order quenching rate constant and quencher exit rate constant, respectively, τ_0 is the fluorescence lifetime in the absence of quenching, and $\langle n \rangle$ is equal to the quencher and micellar molar ratio and is the average number of quencher molecules per micelle or the occupation number. An important assumption is that the probe remains stationary in the same compartment during the observation time. In most studied cases it is valid that $k_q \gg k_-$, leading to $A_2 = 1/\tau_0 + k_e$, $A_3 = \langle n \rangle$, and $A_4 = k_q$. Such simplification implies that probe and quencher distributions are frozen during the fluorescence observation time. By fitting Eq. (2) to the experimental decay curves, one can finally obtain all rate constants and $\langle n \rangle$, from which the micellar aggregation number N_M can be determined from

$$N_M = \langle n \rangle / X = \langle n \rangle ([S] - CMC)/[\text{quencher}] \tag{3}$$

where X is the mole fraction of quenchers in the micelles, [S] the surfactant concentration, and CMC the critical micelle concentration.

Two-dimensional diffusion of amphiphiles in phospholipid [dimyristoyl phosphatidylcholine (DMPC), dipalmitoyl phosphatidylcholine (DPPC)] monolayers at the air-water interface has been determined by studying the fluorescence quenching of pyrene-labeled phospholipid [pyrene–dipalmitoyl phosphatidylethanolamine (DPPE)] (9). Without the presence of quencher, the fluorescence decay of pyrene-DPPE was found to be exponential, which indicates a homogeneous distribution of probe lipid over the two-dimensional lipid surface. Addition of quencher to the monolayer produced a nonexponential decay. The experimental decay could be adequately described by diffusion-controlled quenching in a two-dimensional environment.

A few remarks concerning TRFQ should be made. In most cases studied, the technique is not the only applied one but is complemented by other methods such as viscosimetry, conductivity, potentiometry, self-diffusion measurements, light scattering, calorimetry, or electron microscopy (cryo–transmission electron microscopy, TEM) to provide a full characterization of the system and to check hypotheses concerning the size and shape of the aggregates. In order to apply TRFQ in a strict sense, the micelles should have a spherical or spheroidal shape. Cryo-TEM has shown to be a powerful tool to provide the morphology of surfactant systems and to decide whether TRFQ can be safely applied (10). A more advanced TRFQ model accounting for rodlike micelles has been described (11). The same research group also made a critical assessment of TRFQ in a nonideal mixed micellar system in which the apparent aggregation number significantly deviates from the true one (12).

B. Time-Resolved Fluorescence Anisotropy

Time-resolved fluorescence anisotropy (TRFA) is a technique capable of detecting motional behavior of probe molecules in macromolecules (see Fig. 3) and bilayer membranes (see Fig. 4). In the case of bilayer membranes, probe molecules often have a cylindrical shape. From TRFA, information can be retrieved about the order and reorientational dynamics of these symmetric probes embedded in membranes. In addition, changes in membrane structure or the occurrence of interactions with proteins can be followed when these parameters are changing. The fluorescence anisotropy is defined as

$$r(t) = \frac{I_{\parallel}(t) - I_{\perp}(t)}{I_{\parallel}(t) + 2I_{\perp}(t)} = \frac{I_{\parallel}(t) - I_{\perp}(t)}{F(t)} \tag{4}$$

where $I_{\parallel}(t)$ and $I_{\perp}(t)$ are the parallel and perpendicular polarized fluorescence intensity decays and $F(t)$ is the total fluorescence decay, from which the fluorescence lifetime(s) is (are) obtained. Equation (4) can be written in a form so that it is immediately apparent that one is dealing with the motion of the emission transition moment μ_e:

$$r(t) = \langle P_2[\mu_a(0)\mu_e(t)] \rangle \tag{5}$$

$P_2(x)$ has the form of a second-order Legendre polynomial, μ_a is the direction of the absorption transition moment at $t = 0$, and the brackets $\langle \cdot\cdot \rangle$ denote an ensemble average. When there is no motion at all, $r(t)$ becomes

$$r(t) = r_0 = \tfrac{2}{5} P_2(\cos \delta) \tag{6}$$

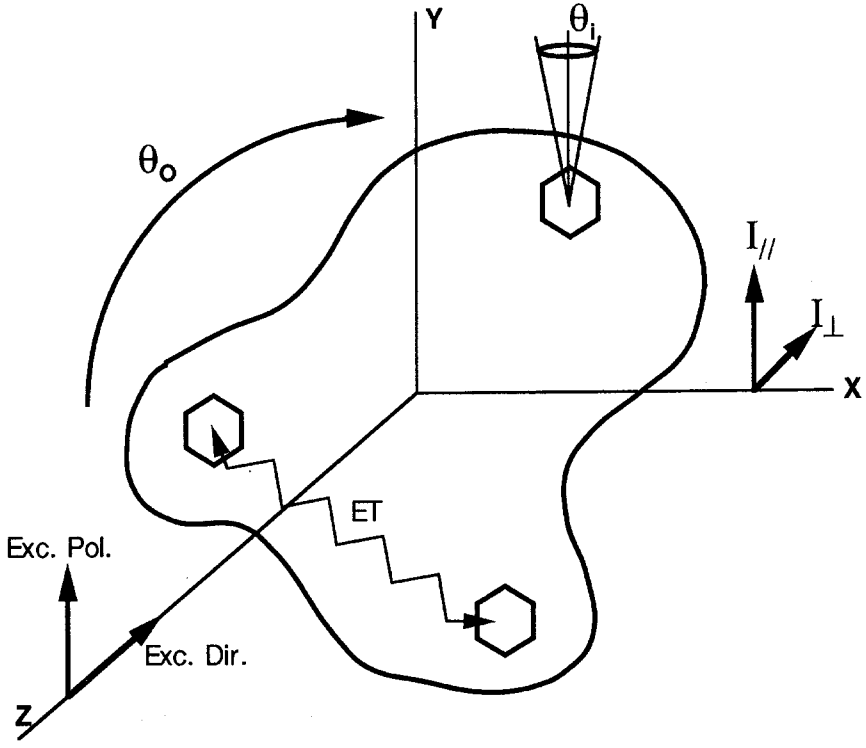

Fig. 3 Fluorescence anisotropy is measured by determining the (normalized) difference between fluorescence that is polarized parallel ($I_{\parallel}$) and that is polarized perpendicular ($I_{\perp}$) with respect to the polarization direction of the excitation light (see text). Fluorescence anisotropy can be initiated by local flexibility (θ_i) of the part of the molecule where the excited chromophore is situated, as well as by movement (θ_o) of the complete molecule. In addition, fluorescence anisotropy can be initiated by internal energy transfer (ET). The contributions of the different origins of fluorescence anisotropy can be separated by changing experimental parameters such as sample temperature or the wavelength of excitation and/or detection.

where r_0 is the fundamental anisotropy and δ the angle between absorption and emission transition dipole moments. If there are two rotational diffusion processes occurring on different time scales, Eq. (5) can be factorized in three terms:

$$r(t) = r_0 C_x(t) C_y(t) \tag{7}$$

where $C_x(t)$ and $C_y(t)$ are the correlation functions of two independent rotational diffusion processes.

For studies of phospholipid membranes the most popular probe has been (and still is) the rod-shaped 1,6-diphenyl-1,3,5-hexatriene (DPH), its charged derivative TMA-DPH (trimethylammonium-DPH), and the phosphatidylcholine (PC) analogue DPH-PC. From TRFA studies one can obtain information on the orientational order and restricted rotational dynamics of the DPH cylinder in phospholipid bilayer

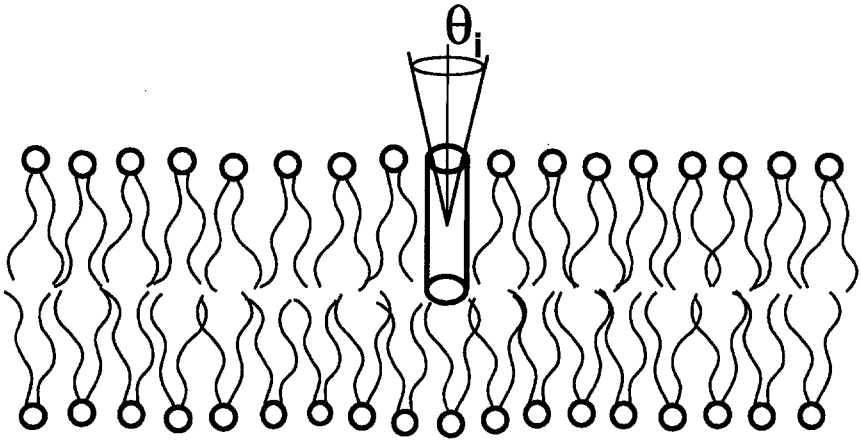

Fig. 4. When a chromophore is incorporated in a lipid bilayer, the fluorescence anisotropy of the chromophore originates from reorientation movements (θ_i) of the chromophore within the bilayer. The movement of the complete bilayer is beyond the nanosecond time scale of fluorescence and is found as a quasi-stead-state value in the experimental data of the anisotropy decay.

membranes such as vesicles. The rotational behavior [or one of the correlation functions in Eq. (7)] of the DPH cylinder in a membrane system can be adequately modeled using the concept of Brownian diffusion of the probe in an orienting potential (13,14). In most comparative TRFA investigations on membrane systems, relatively simple concepts such as the orientational order parameter S are used:

$$S = \sqrt{\frac{r_\infty}{r_0}} \tag{8}$$

where r_∞ is the residual anisotropy at the end of the observation time window. The average fluorescence lifetime of DPH is rather sensitive to the polarity of its immediate environment. Therefore comparative studies deal with the analysis of both $F(t)$ and $r(t)$. The effects studied are, among others, hydration as a function of degree of lipid unsaturation and sterol addition to lipid bilayers.

Another interpretation of TRFA was presented for DPH localized in two distinct populations in lipid vesicles (15). The first population was found to arise from DPH molecules residing in the core of the membranes with an orientation parallel to the membrane normal, while the other population was located at the interface with an average orientation perpendicular to the interface.

The TRFA of DPH-PC and DPH-DG (DPH-diacylglycerol) in dioleoyl phosphatidylcholine (DOPC) vesicles has been compared (16) (see Fig. 5). The TRFA of DPH-DG decays to a lower r_∞ value than that of DPH-PC, indicating a lower degree of ordering of the neighboring lipid chains experienced by DPH-DG. The lack of the phosphocholine headgroup in DG apparently induces a packing failure of close fit to the neighboring PC lipids. DPH-DG is a specific substrate for protein kinase C (PKC). Under optimum conditions for association of PKC to DOPC vesicles,

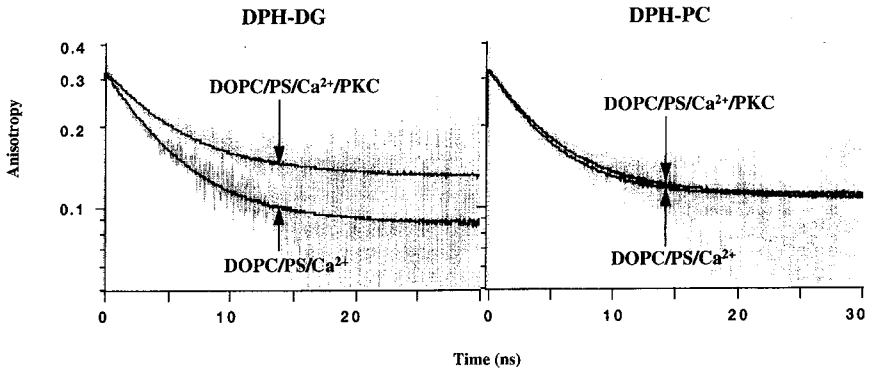

Fig. 5. Experimental and fitted fluorescence anisotropy decays of DPH-DG (left) and DPH-PC (right) in DOPC vesicles (containing brain PS in a DOPC/PS molar ratio of 4:1; total lipid concentration 15 μM) and either DPH-DG or DPH-PC (molar ratio of labeled lipid to unlabeled lipid = 1:150) and in the presence of 0.5 mM calcium. The temperature was 293 K. The buffer used was 20 mM Tris-HCl, 120 mM NaCl, pH 7.4. The fitted decays correspond to the optimal fit with a general diffusion model assuming a Gaussian orientation distribution. In the absence of protein kinase C (PKC) there is a distinct difference in the orientation distribution of both DPH lipids. DPH-PC is oriented with smaller angle (0.60 rad) to the membrane normal than DPH-DG (0.65 rad). When 0.4 μM PKC is present, DPH-DG is selectively bound to PKC, leading to less motional freedom and a smaller angle (0.54 rad). The control lipid DPH-PC is not bound to PKC. (Adapted from Ref. 16.)

DPH-DG is bound to PKC, which leads to a raise in r_∞ value to a similar level as for DPH-PC. The TRFA then becomes indistinguishable from that of the control lipid DPH-PC, which does not interact with PKC.

The interaction of the channel-forming peptide gramicidin A with a wide range of bilayer vesicles has been studied with TRFA of TMA-DPH and DPH-PC (17) and with DPH (18). The nonchannel gramicidin conformation has an ordering effect on DPH in the bilayer, which lacks the channel conformation. An example of the application of other probes (in combination with DPH) is the use of the polarity probe dansyl-phosphatidylethanolamide (dansyl-PE), in conjunction with orientational order determinations using DPH-PC, to monitor hydration near the phospholipid headgroup (19). The membranes were composed of PC, but with acyl chains having varying degree of unsaturation either on the *sn*-2 chain or on both *sn*-1,2 chains.

Other investigations describe the combination of pyrene-PC with DPH probes (20,21). TMA-DPH is used as a surface probe to monitor the changes in fluorescence lifetime and rotational dynamics when cholesterol and β-sitosterol are incorporated in dipalmitoyl phosphatidylcholine (DPPC) bilayer vesicles or when measurements are performed below and above the phase transition temperature (20). Pyrene in Pyr-PC is located in the hydrophobic interior and registers lifetime and rotational changes upon sterol addition, which are significantly different from those observed via TMA-DPH (20). By measuring lateral diffusion of Pyr-PC in binary mixtures of PE (which tends to form a hexagonal ordered phase H_{II}) and PC in membranes and rotational diffusion of DPH-PC, the onset of packing defects at about 60%

PE in the mixture has been demonstrated (21). The rotational dynamics of DPH-PC in the PE-PC mixed membrane have been modeled using a rod-shaped probe in a curved matrix. TRFA can then be described by Eq. (7), in which $C_x(t)$ is the wobbling diffusion part and $C_y(t)$ the part describing the curvature-associated rotation.

Other reports mention the use of *trans*-parinaric acid as a natural fatty acid membrane probe for the investigation of cholesterol effects on artificial membranes or membranes isolated from blood platelets (22,23). *trans*-Parinaric acid has, like DPH, a more or less rodlike structure. The interaction between a labeled lysophospholipid [nitrobenzdiazole phosphatidylethanolamide (*N*-NBD-PE)] and the bile salt taurodeoxychelate (TDC) has been demonstrated with TRFA at concentrations below the CMC of both components (24). Evidence has been given that the lysophospholipid seeds the aggregation of TDC micelles. Porphyrins have been used as probes to characterize anionic (sodium dodecyl sulfate, SDS), cationic cetyltrimethyl ammonium bromide (CTAB), and nonionic micelles (Triton X-100) in water (25). The TRFA could be described by Eq. (7), where $C_x(t)$ can now be conceived as both rotational and translational diffusion inside the micelles and $C_y(t)$ as overall micelle tumbling. Fluorescence anisotropy decay measurements turn out to be an excellent method for directly observing a protein adsorbed to a hydrophobic latex (Teflon) (26). Because the Teflon particles are much larger than the protein (subtilisin), the TRFA of the tryptophan in subtilisin indicates complete immobilization of adsorbed protein on the observation time scale (15 ns). The TRFA of the protein in solution decays to zero.

A warning should be given in the case of fluorescence anisotropy decay investigations of pyrene-containing phospholipids in bilayer membranes. They should be only qualitatively interpreted. Some experiments using two different pyrene-labeled phopholipids DOPC vesicles and erythrocyte ghosts are described in Ref. 27. It can be clearly shown that the properties of pyrene are not so suitable here, because the fluorescence lifetime of pyrene is an order of magnitude longer than the reorientational dynamics of the probe in both membranes and the initial anisotropy (r_0) is rather low ($r_0 \approx 0.2$). In addition, the theoretical treatment of the rotational motion is extremely complex (see Ref. 13). In DOPC vesicles the fluorescence anisotropy of both pyrene lipids declines to zero at longer times (20 ns). This indicates that the rotation of the pyrene chains is not restricted on the time scale of the relatively long fluorescence lifetime (150 ns). However, in the protein-rich ghost cells, the fluorescence anisotropy of one of the lipids has a finite value at longer times (20 ns), indicating that its motion is restricted. In this particular case the acyl chains are apparently interacting with the protein surface. The control pyrene lipid is not restricted in its motions in the ghost membranes.

An interesting study of the distribution of hydrophobic probe molecules in lipid bilayers of palmitoyloleoyl phosphatidylcholine (POPC) vesicles was presented, where TRFA measurements were combined with Monte Carlo dynamics computer simulations (MCDCS) (28,29). It is found that with perylene (TRFA and MCDCS) and DPH (MCDCS) in the lipid bilayer two distinct orientational populations exist, in agreement with the two distinct environments of the middle of the bilayer and in regions near the bilayer interface. Ambiguities were found in comparing the results of TRFA and MCDCS. It was concluded that TRFA on macroscopically unoriented samples will not provide sufficient information for a full characterization of the orientational distribution of probe molecules in bilayers.

The long-lived fluorescence of coronene has been used as a probe for investigating submicrosecond lipid dynamics in DPPC bilayer membranes (small unilamellar vesicles, SUVs), below and through the gel-to-liquid crystalline phase transition (30). TRFA at increasing temperatures showed three rotational decay components: long correlation times of coronene located in a gel-like lipid phase, short correlation times representative of coronene in fluidlike regions, and intermediate correlation times characteristic of a coronene environment arising from fluidization of gel lipid. A Landau adapted expression for describing gated packing fluctuations has been developed, that could adequately describe both thermodynamics and (rotational and diffusion) kinetics of the anisotropy data.

C. Fluorescence Decay Measurements

The determination of fluorescence lifetimes of lipid probes in membranes systems has provided detailed insight into microenvironmental effects resulting from changes in membrane structure or phase. The most frequently used probes are DPH, pyrene-containing lipids, and NBD-lipids. In the following, the properties of these lipid probes in different membranes will be discussed. The remainder of this section is then devoted to some properties of a natural antibiotic molecule that possesses intrinsic fluorescence similar to that found in *trans*-parinaric acid and of fluorescent molecules that are characterized by a twisted intramolecular charge transfer (TICT) state.

As already stated in the previous section, the fluorescence lifetime (and quantum yield) of DPH is strongly dependent on the polarity of its microenvironment. This has been investigated for DPH and TMA-DPH in egg phosphatidylcholine vesicles in normal and deuterated water, the latter showing a dielectric constant 12% lower than that of normal water (31). The fluorescence decay was analyzed using a Lorentzian lifetime distribution. A decrease of the dielectric constant along the membrane normal shifts the centers of the distribution to longer lifetimes and sharpens the widths of the distribution. The addition of cholesterol results in a further shift and narrowing. The profile of the dielectric constant along the membrane normal turns out to be nonlinear.

Pyrene-containing lipids dispersed in membranes have been widely used to probe two-dimensional lateral diffusion in membranes via the propensity of pyrene for excimer formation. The application of a diffusion-controlled bimolecular reaction theory in two dimensions to fit the time-resolved monomer and excimer fluorescence intensity data results in very consistent values for the diffusion coefficient and monomer and excimer fluorescence lifetimes of pyr_{10}-PC(1-palmitoyl-2-(1-pyrenodecanoyl)-*sn*-glycero-3-phosphatidylcholine) in POPC multilamellar vesicles in the fluid phase (32). The diffusion coefficient (e.g., $D = 3.1 \times 10^{-12}\,m^2\,s^{-1}$ at 25°C) and diffusion activation energy ($E_a = 35\,kJ\,mol^{-1}$) obtained are in good agreement with the results of other techniques.

A Langmuir-type film balance was equipped with a fluorescence microscope for time-resolved fluorescence monitoring of membrane dynamics using pyrene excimer formation (33). The monolayers consisted of DMPC and the pyrene probe was attached to a lecithin. The fluorescence decay of the monomer-forming excimers was modeled in terms of the Smoluchowski theory for two-dimensional fluids. It is shown that the time course of excimer formation is strongly determined by a

time-dependent association rate constant. The variation of lateral diffusion with lipid packing density has been measured and compared with theoretical predictions.

The important advantage of dipyrenyl lipids over monopyrenyl lipids is that excimer emission is formed at an extremely low probe-to-lipid molar ratio. A systematic fluorescence study of dipyr$_n$-PC (n from 4 to 14) in DOPC (L_a phase) or DOPE (L_a or H_{II} phase depending on temperature) has been performed (34). The fluorescence dynamics of monomer and excimer emission were found to exhibit a chain length dependence in normal and curved bilayers. The internal dynamics of the pyrenyl chains could be modeled with a lattice model.

The photophysical properties of NBD attached to the *sn*-2 acyl chain of various phospholipids [PC, PE, phosphatidylserine (PS), phosphatidic acid (PA)] or to the PE headgroup and inserted into vesicles of PC, phosphatidylglycerol (PG), PA, or PS have been investigated (35). For various couples of probe and host lipids, the authors observed that the fluorescence decay was dominated by an increase in the nonradiative decay constant k_{nr}. NBD did exhibit a strong solvatochromism, and by comparing the fluorescence properties of *N*-propylamino-NBD in a set of organic solvents it was shown that NBD in the lipid environment experiences a dielectric constant of around 27–41, corresponding to a medium of rather high polarity found in the headgroup region. The fact that the fluorescence decay of NBD is very dependent on changes in k_{nr} renders the fluorescence very sensitive to thermal changes. This property of NBD-conjugated lipids (PC, PE) has prompted researchers to apply these lipids as optical thermometers in the membranes of living cells (36). When the NBD probe-to-phospholipid molar ratio is chosen relatively high (1–50 mol %), NBD molecules aggregate in the membrane, which leads to self-quenching of the fluorescence. An empirical model has been developed that accounts for changes in fluorescence lifetime and quantum yield of NBD with the fractional concentration of incorporated NBD-PE in the membrane matrix (egg phosphatidylcholine, soya bean L-α-lecithin, DPPC, DPPA) (37).

The self-association of the natural fluorescent antibiotic nystatin in gel-phase DPPC vesicles was demonstrated with time-resolved fluorescence techniques (38). In contrast to NBD-PE, nystatin exhibits no self-quenching of the fluorescence when it aggregates. The contribution of a long decay component of 33 ns increases, which was explained by a more rigid environment of the nystatin aggregates in the bilayer. Nystatin (which is supposed to form pores in a membrane bilayer) is more preferably partitioned in the gel phase than in the liquid crystalline phase.

A new method for the analysis of physicochemical properties of liquid water near surfaces [such as water entrapped in AOT reverse micelles (aerosol-OT or dioctylsulfosuccinate)] has been described (39). Fluorescent probe molecules were dissolved in the water phase. The ability of the probe to undergo nonradiative transitions after excitation with picosecond laser pulses depended on the reorientational relaxation time of the water: It can be orders of magnitude slower when the water is bound to the interface. It was possible to observe direct competition between probe diffusion and the nonradiative event and to determine both rates as a function of the distance of the probe from the interface.

The polarity probes Prodan and Patman have been incorporated into phospholipid vesicles with the aim of monitoring solvent relaxation (from time-resolved emission spectral shifts) at different depths in the bilayer (40). It was shown

that Patman is localized deeper in the membrane and senses a less polar and more restricted probe environment.

TICT state fluorescent probes have been introduced in membranes and their time-resolved fluorescence properties studied. The potential-sensitive fluorescent styryl dye RH421 (*N*-(4-sulfobutyl)-4-(4-(*p*-dipentylaminophenyl)-butadienyl)-pyridinium inner salt), dissolved in organic solvents, cationic cetyltrimethyl ammonium chloride (CTAC), or anionic STS (sodium tetradecyl sulfate) micelles, is an example that exhibits can excited-state reaction because an initial rise in the fluorescence is observed in the red part of the emission spectrum (41). The results are discussed in terms of the formation of a fluorescent TICT state occurring simultaneously with the relaxation of the surrounding solvent cage. The effect of an intramembrane electric field on the photophysical properties of the same dye has been investigated by the binding of the hydrophobic ion tetraphenyl borate (TPB) to DMPC vesicles (42). TPB was found to increase significantly the average fluorescence lifetime, which is consistent with reorientation of the dye farther into the membrane interior.

The mesostructure of evaporated porphyrin films was studied, combining fluorescence decay measurements with atomic force microscopy, confocal fluorescence microscopy, and near-field scanning optical microscopy (NSOM) (43). On evaporation of the solvent, a thin film with rings of porphyrins (wheels) was formed on different substrates. It was found that the structure, size, and perfection of these rings depend mainly on the solvent ($CHCl_3$, CCl_4, MeOH, and mixtures of them) and the substrate (glass and graphite). The rings were composed of porphyrin molecules in a locally aggregated configuration, which was formed prior to complete evaporation of the solvent.

One technique of growing interest for probing molecular interactions at interfaces is time-resolved evanescent wave induced fluorescence spectroscopy (TREWIFS) (44). Using TREWIFS, the adsorption behavior of fluorescently labeled bovine serum albumin was studied as a function of penetration depth and concentration of adsorbed protein. The fluorescence kinetics strongly depend on the surface concentration of adsorbed protein. Hydrophilic and hydrophobic surfaces induced different effects, which were ascribed to either higher surface coverage or a closer packed protein structure.

D. Fluorescence Resonance Energy Transfer

Förster-type fluorescence resonance energy transfer (FRET) between a suitable chromophoric donor-acceptor pair has been extensively used as a "spectroscopic ruler" in self-assembly systems such as micelles, vesicles, and monolayers. Distance measurements using FRET are possible because the efficiency of energy transfer from donor to acceptor depends on the inverse sixth power of the donor-acceptor distance. The concepts of FRET in macromolecular assemblies were developed at the end of the 1970s (45–47). Depending on the nature of the applied donor-acceptor pair, the applicable range is between 1.0 and 5.0 nm (long range!), which spans more than the diameter of a bilayer membrane.

The theory of radiationless energy transfer was formulated by Förster (48). Important to note is that donor and acceptor molecular dipoles are very weakly interacting, meaning that they cannot be nearest neighbors in a self-aggregated system.

Förster has derived the following expression for the rate constant of transfer k_T:

$$k_T = 8.71 \times 10^{23} R^{-6} J \kappa^2 n^{-4} k_f \ (s^{-1}) \tag{9}$$

where R is the donor-acceptor distance, n the refractive index, k_f the radiative fluorescence rate constant, and J the overlap integral ($M^{-1}\,cm^3$), which is the degree of spectral overlap between donor fluorescence and acceptor absorption given by

$$J = \int_0^\infty F_D(\lambda)\varepsilon_A(\lambda)\lambda^4 \, d\lambda \tag{10}$$

where F_D is the normalized fluorescence spectrum of the donor (in such a way that $\int_0^\infty F_D(\lambda)\, d\lambda = 1$) and $\varepsilon_A(\lambda)$ is the extinction coefficient at wavelength λ. The so-called orientation factor κ^2 is

$$\kappa^2 = [\cos\theta_T - 3\cos\theta_D \cos\theta_A]^2 \tag{11}$$

where θ_D and θ_A are the angles between the emission transition moment of the donor and the absorption transition moment of the acceptor, respectively, and the donor-acceptor separation vector; θ_T is the angle between donor-acceptor transition moments.

The orientation factor in energy transfer is, for "unknown" systems, the indeterminate parameter in Eq. (9); all other parameters can be measured or evaluated. Furthermore, many proteins contain more than one donor or acceptor molecule. Dale and coworkers (49) have critically evaluated the possible cases encountered in biopolymers. For details we refer to the original paper. All factors in Eq. (9), except the distance, can be lumped together in the so-called critical transfer (or Förster) distance R_0:

$$R_0 = 9.79 \times 10^3 (\kappa^2 n^{-4} Q_D^0 J)^{1/6} \ (\text{Å}) \tag{12}$$

where Q_D^0 is the quantum yield of donor fluorescence in the absence of acceptor molecules and the superscript 0 denotes the absence of acceptor (note that $Q_D^0 = \tau_D^0/\tau_{D_r}^0$ where $\tau_{D_r}^0$ is the radiative lifetime and τ_D^0 the actual lifetime). The critical transfer distance is defined as the distance at which the transfer rate is equal to the donor fluorescence decay rate. Now Eq. (9) can be simplified to

$$k_T = \frac{1}{\tau_D^0}\left(\frac{R_0}{R}\right)^6 \tag{13}$$

The actual distance R between a donor and an acceptor can be determined by measuring the transfer efficiency E:

$$E = 1 - \frac{\tau_D}{\tau_D^0} = 1 - \frac{Q_D}{Q_D^0} \tag{14}$$

Thus, relative fluorescence lifetime or quantum yield measurements of the donor, in the absence and presence of the acceptor, will yield the efficiency of energy transfer. This

experimental efficiency can be directly related to the distance R via

$$E = \frac{k_T}{(\tau_D^0)^{-1} + k_T} = \frac{R_0^6}{R_0^6 + R^6} \tag{15}$$

One practical drawback is that the donor fluorescence parameters in the absence of acceptor are always needed. This means that in proteins with natural donor-acceptor pairs the acceptor needs to be removed to have the fluorescence decay or intensity parameters in the absence of the acceptor.

In artificial membranes the donor-acceptor couples are usually lipophilic and are assumed to be uniformly distributed over both leaflets of the bilayer. In biological membranes, a significant fraction of membrane area is occupied by proteins and the assumption of a uniform lipid probe distribution is no longer valid in these crowded membranes. Zimet et al. (50) considered the situation of a fluorescent donor linked to a membrane protein and lipid-like acceptor molecules partitioned over both leaflets but excluded from the protein area. Monte Carlo simulations were used to generate donor and acceptor distributions that were linked numerically to FRET equations that determine the spectroscopic observables: the average donor quantum yield and fluorescence lifetime distribution as function of protein area fraction (up to 50%).

The problem of electronic energy transfer among chromophores randomly distributed within monodisperse micelles has been addressed (51). Because the energy transfer dynamics are well described by a superposition of pairwise interactions, the pairwise distribution function has been modeled under given geometric constraints and related to macroscopic FRET observables. Different types of energy transfer, application to concentrated micelles, and dynamic and static orientational averaging limits have been discussed in the developed model.

Both experimental and theoretical approaches have been followed to obtain information about the geometry of bilayers formed in nonionic surfactant aqueous dispersions (mixed membranes of POPC/$C_{12}EO_n$ with $n = 1$–8 ethylene oxide units) (52). Depending on the n value, nonlamellar structures ($n < 5$) or mixed micelles ($n > 5$ corresponding to a tendency to solubilize the membrane) are formed. In these mixed membranes the donor is NBD-PE and the acceptor is rhodamine-PE and both donor and acceptor molecules are assumed to be uniformly distributed. From FRET experiments and analyses, the surface area of the lamellae is determined and the area per detergent is found to increase with larger number of EO units. The area is expressed in terms of a critical packing parameter yielding a measure of the asymmetry of the membrane shape.

A purely experimental FRET approach has been developed to analyze the distance between several lipopolysaccharides (LPSs) of different molecular masses equipped with fluorescein isothiocyanate (FITC) as donor and two different lipophilic acceptor molecules (yielding two different critical transfer distances R_0 as internal standard) in sulfobetaine palmitate micelles (53). The short-chain FITC-LPS is located at the micellar surface, and the long-chain FITC-LPS is extended outside the micelle at a distance of $1.5R_0$ or more.

Quantitative studies of the binding of PKC to lipid cofactors in a membrane-mimetic system by monitoring resonance energy transfer have been described (54). For that purpose different headgroup lipids were labeled with a pyrenyl

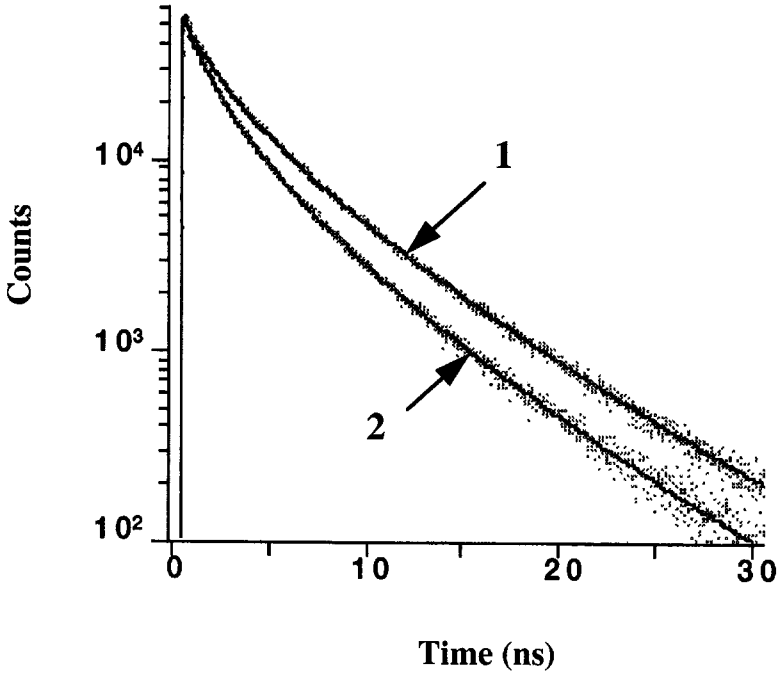

Fig. 6. Experimental and fitted decays of tryptophan fluorescence of 80 nM protein kinase C (PKC) in buffer (curve 1) and in the presence of 100 μM thesit [poly(oxyethylene)-9-lauryl ether] containing 5 mol % PS and 4 mol % pyrPIP$_2$ (*sn*-2-pyrenyldecanoyl-phosphatidylinositol-4,5-bisphosphate) (curve 2). The temperature was 293 K. The buffer used was 20 mM Tris-HCl, 50 mM KCl, and 1 mM calcium, pH 7.5. The fitted curves represent the fit to a lifetime distribution recovered with the maximum entropy method of analysis. Because PKC binds selectively to pyrPIP$_2$ in the thesit micelle, energy transfer from the tryptophan residues in PKC to pyrPIP$_2$ occurs, resulting in faster fluorescence decay than that in the absence of micelles. (From Ref. 54.)

decanoyl moiety at the *sn*-2 position of the lipid glycerol. These labeled lipids proved to be excellent energy acceptors of light-excited tryptophan residues in PKC. The quenching efficiency of the tryptophan fluorescence was determined as a function of lipid probe concentration in mixed micelles consisting of poly(oxyethylene)-9-lauryl ether, PS, and various mole fractions of probe lipid. The analysis of the progressively faster decaying tryptophan fluorescence in PKC allowed estimation of the binding constants of pyrene lipids to PKC (Figs. 6 and 7). Only the lipids that were also found to activate PKC in the standard enzymatic assay exhibit high affinity for PKC. In the latter case PKC is bound to the mixed micelle and energy transfer from the tryptophan residues to the pyrene acceptor can take place.

The antibiotic nystatin (see also Ref. 38) is also a good energy acceptor of tryptophan fluorescence, and its interaction with yeast plasma membranes has been investigated with FRET in order to assess whether membrane proteins interact with nystatin in the presence of ergosterol (55).

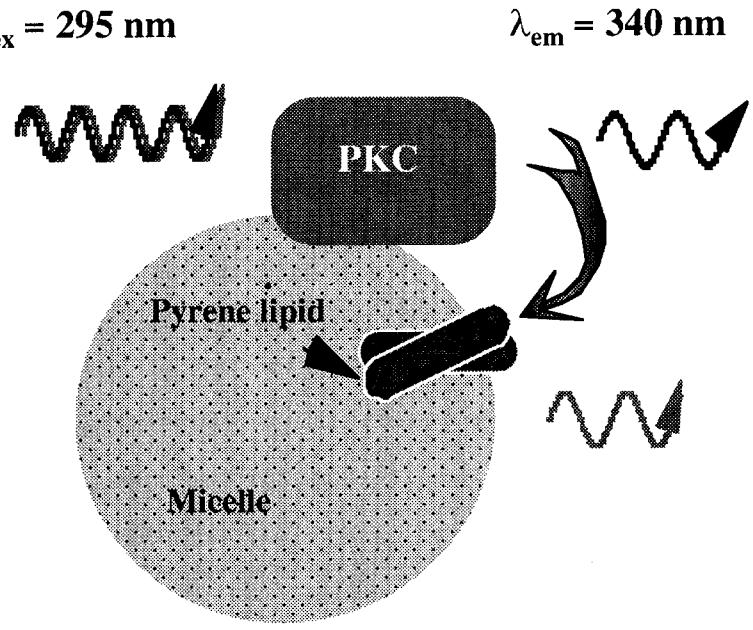

Fig. 7. Cartoon presentation of the binding experimnent in Fig. 6. When PKC selectively binds to the headgroup of a particular pyrenyl-phospholipid, the tryptophan residues in PKC will be close to or within the critical transfer distance (2.7 nm) of the tryptophan-pyrene pair and radiationless energy transfer from tryptophan residues to pyrene can occur, leading to faster tryptophan fluorescence decay. The diameter of PKC is about 6 nm and the diameter of the micelle about 7 nm. A pyrenyl-phospholipid that does not interact with PKC would be distributed over the micelle and energy transfer would be much less probable.

E. Multiphoton Excitation

Multiphoton excitation or MPE (56) can be used to excite molecules more selectively, both in spectral sense and spatially (57). It is a spectroscopic technique in which the energy of two (or more) photons is required for absorption by the chromophore. The flux of excitation light toward the molecule must be so high that, on the time scale of absorption (femtoseconds), multiple photons are available to be absorbed. The energy densities necessary for this can be obtained only from ultrashort (femtosecond) high peak power (sub-MW) laser pulses and only when the beam is focused to a micrometer spot. When two-photon excitation (2PE) is applied, the fluorescence yield has a quadratic dependence on the excitation power. On the other hand, the fluorescence yield, compared with the yield of background fluorescence, also has a quadratic dependence on the cross sections of the respective optical densities at half the excitation wavelength. Another important property of multiphoton excitation is the dependence of the fundamental anisotropy (r_0) on the applied transition moment. For reduced nicotinamide adenine dinucleotide (NADH) a 46% increase of the initial polarization was reported (58) in the case of 2PE compared with

one-photon excitation (1PE). This will, of course, enhance the dynamic range and thus the accuracy of fluorescence anisotropy studies. For three-photon excitation (3PE), however, the initial anisotropy for *N*-acetyl tryptophanamide (NATA) was found to be 0.06 and negative, whereas it was 0.13 and positive for the case of 1PE (59). Therefore, different excitation conditions should be considered depending on the requirements of the experiment.

When a laser beam is focused into a sample, the beam travels through a cone, reaches the focal volume, and spreads out in another cone. When 1PE is applied, combined with confocal detection (60), (part of) the fluorescence of the focal point as well as the two cones will be excited and detected (see also Ref. 61). However, when 2PE is applied, the excitation energy density can be tuned in such a way that two-photon absorption can occur only in the very focus of the beam. At other places the energy density is then too low for two-photon absorption. Therefore no absorption and no fluorescence from places other than the focal volume (even smaller than in the case of 1PE) will be observed. Furthermore, Rayleigh scattering and Raman scattering usually have a quite different spectral position compared with a 1PE experiment and can be easily eliminated. In addition, with infrared light deeper penetration depths in biological materials can be obtained. A drawback for MPE can be the risk of continuum generation in the solvent when these high peak energies are applied (62).

The evanescent wave at 770 nm from a femtosecond Ti:sapphire laser was used to excite the calcium probe Indo 1 at a quartz-water interface (63). The fluorescence intensity of Indo 1 depended quadratically on the incident power slightly above and below the critical angle. Scattered light did not contribute to the emission signal. 2PE gave rise to significantly higher anisotropy.

The effect of near-infrared femtosecond lasers on the vitality and reproduction of Chinese hamster ovary cells (730–800 nm, 80 MHz, 80 μs pixel dwell time) has been investigated (64). Cells were unaffected by powers less than 1 mW. The cells did not divide (die or form giant cells) at laser powers > 6 mW and were destroyed at mean powers > 10 mW. Extremely high fields may induce destructive intracellular plasma formation.

MPE at 730 and 960 nm was used to image human skin autofluorescence near the surface (50 μm) or at greater depths (100–150 μm) (65). Using both excitation wavelengths, the fluorescence of reduced pyridine nucleotides (730 nm) and flavoproteins (960 nm) could be identified.

As already indicated, a number of MPE applications have been carried out in the past few years. An increasing number of applications can be foreseen because of the challenging possibilities in many fields of the biological sciences. The commercial availability of femtosecond pulsed lasers in the near-infrared wavelength region as well as complete microscope setups with 2PE will certainly catalyze MPE applications in biological interfaces.

F. Time-Resolved Single-Molecule Fluorescence

In the past few years, a number of different optical spectroscopic techniques have been developed that can be summarized as single-molecule spectroscopy. One goal of that idea is to isolate the molecule in such a way that the spectroscopic properties are not perturbed by the environment or are disturbed only in a well-described way. Furthermore, there has always been a quest for ultimate sensitivity in order to study

the smallest amounts of material. There are in principle two directions to go in for exciting only a single molecule. These are to decrease the volume of excitation (MPE or near- or far-field excitation) and to decrease the concentration of chromophores. Only a few single-molecule techniques have been applied for time-resolved fluorescence studies of interactions of molecules with vesicles, membranes, or artificial interfaces but it is expected that many applications will be developed in the near future.

In scanning near-field optical microscopy (NSOM) the measured fluorescence lifetime of a single dye molecule can be shortened or lengthened depending on the distance between the molecule and an aluminum-coated fiber tip (66). The lifetime variations can be simulated and the computations provide insight into the spectroscopic properties in front of a metal-dielectric interface of arbitrary geometry.

Macklin et al. (67) applied far-field microscopy to probe the optical properties of single dye molecules at a polymer-air interface. Because of the isolated nature of the molecule in these experiments, more specific information can be retrieved. Shifts in the fluorescence spectrum and the orientation of the transition dipole moment were correlated with variation of the fluorescence lifetime caused by the frequency dependence of the spontaneous emission rate (in case of spectral shifts) and by the effects of electromagnetic boundary conditions on the fluorescent radiation at the polymer-air interface (in case of dipole orientation effects).

III. CONCLUSIONS

As is evident from this chapter, there are many interesting problems in the field of biological interfaces that can be effectively studied with time-resolved fluorescence techniques. Many specific questions concerning structure and dynamics of interfaces can be answered by the application of the different variations of time-resolved fluorescence techniques. Judging from other chapters in this book, different techniques have their own benefits, leading to information at other structural levels and in other time frames. A complete overview of all possibilities will lead to the most complete description of these interfaces.

ACKNOWLEDGEMENT

Part of this work was supported by the Netherlands Organization for Scientific Research (NWO). Dr. N. V. Visser is kindly acknowledged for preparing the figures.

REFERENCES

1. A Carrington, AD McLaughlan. Introduction to Magnetic Resonance. London: Harper, 1967.
2. JI Steinfeld. Molecules and Radiation. An Introduction to Modern Molecular Spectroscopy, New York: Harper & Row, 1974.
3. JR Lakowicz. Principles of Fluorescence Spectroscopy. New York: Plenum, 1983.
4. JR Lakowicz, ed.: Topics in Fluorescence Spectroscopy. Parts 1–4. New York: Plenum, 1991–1994.
5. RP Haugland. Handbook of Fluorescent Probes and Research Chemicals. 6th ed. Eugene, OR: Molecular Probes, 1996.
6. AJWG Visser. Time-resolved fluorescence on self-assembly membranes. Curr Opin Colloid Interface Sci 2:27, 1997.

7. PP Infelta, M. Grätzel, JK Thomas. Luminescence decay of hydrophobic molecules solubilized in aqueous micellar systems. A kinetic model. J Phys Chem 78:190, 1974.
8. M Tachiya. Application of a generating function to reaction kinetics in micelles. Kinetics of quenching of luminescent probes in micelles. Chem Phys Lett 33:289, 1975.
9. F Caruso, F Grieser, PJ Thistlewaite, M Almgren. Two-dimensional diffusion of amphiphiles in phospholipid monolayers at the air-water interface. Biophys J 65:2493, 1993.
10. D Danino, Y Talmon, R Zana. Alkanediyl- α,ω-bis(dimethylalkylammonium bromide) surfactants (dimeric surfactants). 5. Aggregation and microstructure in aqueous solutions. Langmuir 11:1448, 1995.
11. M Swanson-Vethamuthu, M Almgren, G Karlsson, P Bahadur. Effect of sodium chloride and varied alkyl chain length on aqueous cationic surfactant–bile salt systems. Cryo-TEM and fluorescence quenching studies. Langmuir 12:2173, 1996.
12. M Almgren, P Hansson, K Wang. Distribution of surfactants in a nonideal mixed micellar system. Effect of a surfactant quencher on the fluorescence decay of solubilized pyrene. Langmuir 12:3855, 1996.
13. C Zannoni, A Arcioni, P Cavatorta. Fluorescence depolarization in liquid crystals and membrane bilayers. Chem Phys Lipids 32:179, 1983.
14. A Szabo. Theory of fluorescence depolarization in macromolecules and membranes. J Chem Phys 81:150, 1984.
15. UA van der Heide, G van Ginkel, YK Levine. DPH is localised in two distinct populations in lipid vesicles. Chem Phys Lett 253:118, 1996.
16. EHW Pap, M Ketelaars, JW Borst, A van Hoek, AJWG Visser. Reorientational properties of fluorescent analogues of the protein kinase C cofactors diacylglycerol and phorbol ester. Biophys Chem 58:255, 1996.
17. JM Muller, G van Ginkel, E van Faassen. Effect of gramicidine A on structure and dynamics of lipid vesicle bilayers. A time-resolved fluorescence depolarization study. Biochemistry 34:3092, 1995.
18. JM Muller, G van Ginkel, E van Faassen. Effect of lipid molecular structure and gramicidine A on the core of lipid vesicle bilayers. A time-resolved fluorescence depolarization study. Biochemistry 35:488, 1996.
19. C Ho, SJ Slater, CD Stubbs. Hydration and order in lipid bilayers Biochemistry 34:6188, 1995.
20. C Bernsdorff, R Winter, TL Hazlett, E Gratton. Influence of cholesterol and β-sitosterol on the dynamic behavior of DPPC as detected by TMA-DPH and PyrPC fluorescence. A fluorescence lifetime distribution and time-resolved anisotropy study. Ber Bunsenges 99:1479, 1995.
21. S-Y Cheng, KH Cheng. Detection of membrane packing defects by time-resolved fluorescence depolarization. Biophys J 71:878, 1996.
22. CR Mateo, AU Acuna, JC Brochon. Liquid-crystalline phases of cholesterol/lipid bilayers as revealed by the fluorescence of *trans*-parinaric acid. Biophys J 68:978, 1995.
23. M Velez, MP Lillo, AU Acuna, J Gonzales-Rodriguez. Cholesterol effect on the physical state of lipid multibilayers from the platelet plasma membrane by time-resolved fluorescence. Biochim Biophys Acta 1235:343, 1995.
24. LJ DeLong, JW Nichols. Time-resolved fluorescence anisotropy of fluorescent-labeled lysophospholipid and taurodeoxycholate aggregates. Biophys J 70:1466, 1996.
25. NC Maiti, S Mazumdar, N Periasamy. Dynamics of porphyrin molecules in micelles. Picosecond time-resolved fluorescence anisotropy studies. J Phys Chem 99:10708, 1995.
26. MCL Maste, EHW Pap, A van Hoek, W Norde, AJWG Visser. Spectroscopic investigation of the structure of a protein adsorbed on a hydrophobic latex. J Colloid Interface Sci 180:632, 1996.

27. EHW Pap, A Hanicak, A van Hoek, KWA Wirtz, AJWG Visser. Quantitative analysis of lipid-lipid and lipid-protein interactions in membranes by use of pyrene-labeled phophoinositides. Biochemistry 34:9118, 1995.
28. MAMJ van Zandvoort, HC Gerritsen, YK Levine. Distribution of hydrophobic molecules in lipid bilayers. 1. Monte Carlo dynamics simulations. J Phys Chem B 101:4142, 1997.
29. MAMJ van Zandvoort, HC Gerritsen, G van Ginkel, YK Levine, R Tarroni, C Zannoni. Distribution of hydrophobic molecules in lipid bilayers. 2. Time-resolved fluorescence anisotropy study of perylene in vesicles. J Phys Chem B 101:4149, 1997.
30. L Davenport, P Targowski. Submicrosecond phopholipid dynamics using a long-lived fluorescence emission anisotropy probe. Biophys J 71:1837, 1996.
31. I Konopasek, P Kvasnicka, E Amler, A Kotyk, G Curatola. The transmembrane gradient of the dielectric constant influences the DPH lifetime distribution. FEBS Lett 374:338, 1995.
32. J Martins, WLC Vaz, E Melo. Long-range diffusion coefficients in two-dimensional fluid media measured by the pyrene excimer reaction. J Phys Chem 100:1889, 1996.
33. R Merkel, E Sackmann. Nonstationary dynamics of excimer formation in two-dimensional fluids. J Phys Chem 98:4428, 1994.
34. KH Cheng, P Somerharju. Effects of unsaturation and curvature on the transverse distribution of intramolecular dynamics of dipyrenyl lipids. Biophys J 70:2287, 1996.
35. S Mazères, V Schram, J-F Tocanne, A Lopez. 7-Nitrobenz-2-oxa-1,3-diazole-4-yl–labeled phospholipids in lipid membranes: Differences in fluorescence behavior. Biophys J 71:327, 1996.
36. CF Chapman, Y Liu, GJ Sonek, BJ Tromberg. The use of exogenous fluorescent probes for temperature measurements in single living cells. Photochem Photobiol 62:416, 1995.
37. JDA Shrive, JD Brennan, RS Brown, UK Krull. Optimization of the self-quenching response of nitrobenzoxadiazole dipalmitoylphosphatidylethanolamine in phospholipid membranes for biosensor development. Appl Spectrosc 49:304, 1995.
38. A Coutinho, M Prieto. Self-association of the polyene antibiotic nystatin in dipalmitoylphosphatidylcholine vesicles: A time-resolved fluorescence study. Biophys J 69:2541, 1995.
39. CH Cho, M Chung, J Lee, T Nguyen, S Singh, M Vedamuthu, S Yao, J-B Zhu, GW Robinson. Time- and space-resolved studies of the physics and chemistry of liquid water near a biologically relevant interface. J Phys Chem 99:7806, 1995.
40. R Hutterer, FW Schneider, H Sprinz, M Hof. Binding and relaxation behaviour of Prodan and Patman in phospholipid vesicles: A fluorescence and ^{1}H NMR study. Biophys Chem 61:515, 1996.
41. NV Visser, A van Hoek, AJWG Visser, RJ Clarke, JF Holzwarth. Time-resolved polarized fluorescence of the potential-sensitive dye RH421 in organic solvents and micelles. Chem Phys Lett 231:551, 1994.
42. NV Visser, A van Hoek, AJWG Visser, J Frank, H-J Apell, RJ Clarke. Time-resolved fluorescence investigations of the interaction of the voltage-sensitive probe RH421 with lipid membranes and proteins. Biochemistry 34:11777, 1995.
43. J Hofkens, L Latterini, P Vanoppen, H Faes, K Jeuris, S De Feyter, J Kerimo, PF Barbara, FC De Schryver, AE Rowan and RJM Nolte. Mesostructure of evaporated porphyrin thin films: Porphyrin wheel formation. J Phys Chem B 101:10588, 1997.
44. B Crystal, G Rumbles, TA Smith, D Phillips. Time-resolved evanescent wave induced fluorescence measurements of surface adsorbed bovine serum albumin. J Colloid Interface Sci. 155:247, 1993.
45. L Stryer. Fluorescence energy transfer as a spectroscopic ruler. Annu Rev Biochem 47:819, 1978.
46. RH Fairclough, CR Cantor. The use of singlet-singlet energy transfer to study macromolecular assemblies. Methods Enzymol 48:347, 1978.

47. BK-K Fung, L Stryer. Surface density determinations in membranes by fluorescence energy transfer. Biochemistry 17:5241, 1978.
48. T Förster. Zwischenmolekulare Energiewanderung und Fluoreszens. Ann Phys 2:55, 1948.
49. RE Dale, J Eisinger and WE Blumberg. The orientational freedom of molecular probes. The orientation factor in intramolecular energy transfer. Biophys J 26:161 1979.
50. DB Zimet, BJ-M Thevenin, AS Verkman, SB Shohet, JR Abney. Calculation of resonance energy transfer in crowded biological membranes. Biophys J 68:1592, 1995.
51. AV Barzykin, M Tachiya. Electronic energy transfer in concentrated micellar solutions. J Chem Phys 102:3146, 1995.
52. G Lantzsch, H Binder, H Heerklotz, M Wendling, G Klose. Surface areas and packing constraints in POPC/C12EOn membranes. A time-resolved fluorescence study. Biophys Chem 58:289, 1996.
53. CA Wiström, GM Jones, PS Tobias, LA Sklar. Fluorescence resonance energy transfer analysis of lipopolysaccharide in detergent micelles. Biophys J 70:988, 1996.
54. EHW Pap, PIH Bastiaens, JW Borst, PAW van den Berg, A van Hoek, GT Snoek, KWA Wirtz, AJWG Visser. Quantitation of the interaction of protein kinase C with diacyl glycerol and phosphoinositides by time-resolved detection of resonance energy transfer. Biochemistry 32:13310, 1993.
55. M Opekarova, P Urbanova, I Konopasek, P Kvasnicka, K Strzalka, K Sigler, E Amler. Possible nystatin-protein interaction in yeast membrane vesicles in the presence of ergosterol. A Förster energy transfer study. FEBS Lett 386:181, 1996.
56. WL Peticolas, JP Goldsborough, KE Rieckhoff. Double photon excitation in organic crystals. Phys Rev Lett 10:43 1963.
57. W Denk, JH Strickler, WW Webb. Two-photon laser scanning fluorescence microscopy. Science 248:73, 1990.
58. B Kierdaszuk, H Malak, I Gryczynski, P Callis, JR Lakowicz. Fluorescence of reduced nicotinamides using one and two photon excitation. Biophys Chem 62:1, 1996.
59. I Gryczynski, H Malak, JR Lakowicz, HC Cheung, J Robinson, PK Umeda. Fluorescence spectra properties of troponin C mutant F22w with one, two and three photon excitation. Biophys J 71:3448, 1996.
60. GJ Brakenhoff, P Blom, P Barends. Confocal scanning light microscopy with high aperture immersion lenses. J Microsc 117:219, 1979.
61. EHK Stelzer, S Lindek. Fundamental reduction of the observation volume by detection orthogonal to the illumination axis: Confocal theta microscopy. Opt Commun 111:536, 1994.
62. L Brand, C Eggeling, C Zander, KH Drexhage, CAM Seidel. Single molecule identification of Coumarine 120 by time-resolved fluorescence detection: Comparison of one and two photon excitation in solution. J Phys Chem A 101:4313, 1997.
63. I Gryczynski, Z Gryczynski, JR Lakowicz. Two-photon excitation by the evanescent wave from total internal reflection. Anal Biochem 247:69, 1997.
64. K König, PTC So, WW Mantulin, E Gratton. Cellular response to near infrared femtosecond laser pulses in two-photon microscopes. Opt Lett 22:135, 1997.
65. BR Masters, PTC So. Multiphoton excitation fluorescence microscopy and spectroscopy of in vivo human skin. Biophys J 72:2405, 1997.
66. RX Bian, RC Dunn, XS Xie. Single molecule emission characteristics in near field microscopy. Phys Rev Lett 75:4772 1995.
67. JJ Macklin, JK Trautman, TD Harris, LE Brus. Imaging and time-resolved spectroscopy of single molecules at an interface. Science 272:255, 1996.